

Article

Exposure to Aerosols Emitted from Common Heating Combustion Sources Indoors—The Jordanian Case as an Example for Eastern Mediterranean Conditions

Tareq Hussein ^{1,2,*} , Omar Al-Jaghbeer ³, Nizar Bqour ³, Bilal Zidan ³ and Bashar Lahlouh ³

¹ Environmental and Atmospheric Research Laboratory (EARL), Department of Physics, School of Science, The University of Jordan, Amman 11942, Jordan

² Institute for Atmospheric and Earth System Research (INAR/Physics), University of Helsinki, FI-00014 Helsinki, Finland

³ Department of Physics, School of Science, The University of Jordan, Amman 11942, Jordan; amr8190216@ju.edu.jo (O.A.-J.); nza8180337@ju.edu.jo (N.B.); bla8180859@ju.edu.jo (B.Z.); bashar_lahlouh@ju.edu.jo (B.L.)

* Correspondence: tareq.hussein@helsinki.fi

Abstract: In Jordan, ~61% of total residential energy consumption is consumed by heating spaces using portable kerosene (K) and liquified petroleum gas (LPG) heaters. Here, we evaluated the indoor air quality (IAQ) versus the use of K and LPG heaters inside a test room reflecting the typical conditions of Jordanian dwellings during the winter season. The experimental setup included particle size distribution (diameter 0.01–25 μm) measurements, and we utilized a simple sectional indoor aerosol model (SIAM) to estimate the emission rate and lifetime of the combustion products in the test room. The particle number (PN) concentration during the LPG operation was 6×10^4 – $5.9 \times 10^5 \text{ cm}^{-3}$, depending on the setting at minimum, medium, or maximum. The K heater operation increased with the PN concentrations to a range of 4×10^5 – $8 \times 10^5 \text{ cm}^{-3}$. On average, the particle losses were 0.7 – 1.6 h^{-1} for micron particles (1–10 μm) and 0.8 – 0.9 h^{-1} for ultrafine particles (<0.1 μm). The emission rate from the LPG heater was 1.2×10^{10} – 2.8×10^{10} particles/s (6.6×10^6 – 8.0×10^6 particles/J), and that for the K heater was about 4.4×10^{10} particles/s (1.9×10^7 particles/J). The results call for the immediate need to apply interventions to improve the IAQ by turning to cleaner heating processes indoors.

Keywords: portable heater; liquified petroleum gas; kerosene; emission rate; particulate matter



Citation: Hussein, T.; Al-Jaghbeer, O.; Bqour, N.; Zidan, B.; Lahlouh, B. Exposure to Aerosols Emitted from Common Heating Combustion Sources Indoors—The Jordanian Case as an Example for Eastern Mediterranean Conditions.

Atmosphere **2022**, *13*, 870. <https://doi.org/10.3390/atmos13060870>

Academic Editors: Daniele Contini and Francesca Costabile

Received: 5 May 2022

Accepted: 22 May 2022

Published: 25 May 2022

Publisher's Note: MDPI stays neutral with regard to jurisdictional claims in published maps and institutional affiliations.



Copyright: © 2022 by the authors. Licensee MDPI, Basel, Switzerland. This article is an open access article distributed under the terms and conditions of the Creative Commons Attribution (CC BY) license (<https://creativecommons.org/licenses/by/4.0/>).

1. Introduction

In developed countries, kerosene has been a major household, commercial, and industrial fuel since the mid-19th century. The introduction of electrification and the start of gas fuel usage in the mid-20th century reduced the prevalence of household kerosene heating. In response to rising electricity and central heating prices, portable household kerosene (K) and liquified petroleum gas (LPG) heaters became popular in the early 1980s, because they could be moved from room to another as needed. In developing countries, and limited income communities, K and LPG are the predominant methods of household heating [1–4]. This is because they are cheap and their consumption can be controlled easily.

Usually, K and LPG heaters are operated in indoor spaces that have no chimney vents (i.e., unvented). In cold conditions, these indoor environments have minimal ventilation. Furthermore, in limited-income communities, the ventilation is usually natural and inefficient [5,6]. All these factors combined lead to scenarios of extreme exposure to fuel (K and LPG) combustion products [2,7–15]. There has been growing evidence that such exposure is associated with a range of health effects, such as lung cancer, chronic obstructive pulmonary disease (COPD), low birth weight, cataracts, pneumonia, tuberculosis, eye irritation, and

respiratory infections. [16–23]. This is a clear justification for the efforts to find alternative energy sources, or to utilize new ways of fuel combustion more efficiently and reduce air pollution [1,24–26]. This includes green sources of electricity. To some extent, K can be instantly replaced by LPG, which has a higher combustion efficiency (i.e., complete combustion) than K, resulting in less air pollution.

While in storage conditions, exposure to kerosene or natural gas aerosol or vapor can be on a daily basis in households where K and LPG is used as a source of heating or cooking. Furthermore, it is possible that uncombusted kerosene or natural gas components are present during the heating process, and being emitted in the form of PM. Nevertheless, while there is a large body of evidence about the toxicity of kerosene and natural gas vapor, and about aerosol inhalation and dermal exposure to uncombusted fuel, less is known about the toxicity of the combustion product mixture. This is complicated by the fact that the nature and concentrations of the pollutants emitted can be strongly influenced by the source of combustion. The combustion products of K and LPG can include a vast range of air pollutants [4,7,19,27–36]. This includes particulate matter (PM), elemental carbon (EC), organic carbon (OC), carbon monoxide and dioxide (CO and CO₂), formaldehyde (HCHO), polycyclic aromatic hydrocarbons (PAH), sulfur dioxide (SO₂), nitrogen oxides (NO_x), water vapor (H₂O), and oxidative ions (such as H⁺, SO₄²⁻, NH₄⁺). The amounts of these products emitted into the atmosphere depend on whether the type of combustion is complete or incomplete. Numerous studies have demonstrated that heater design (radiant or convective) is influential on emissions of pollutants [5,37–45]. The grade of the fuel is also an important parameter affecting pollutant emissions from heaters.

There seems to have been little research conducted on the exposure implications of household K and LPG combustion [5,40,44,46]. For example, the average CO level in mobile homes using K heaters was in the range of tens mg/m³, which is approximately seven times greater than in homes without K and LPG heaters [7,46,47]. Field measurements have confirmed that kerosene heaters increase indoor concentrations of NO₂, SO₂, PM_{2.5}, and PM₁₀ above ambient levels [4,46–49]. Although most of the investigations were performed more than 20 years ago, more recent studies suggest that improvements in emissions have not been significant [7,38,45].

In this study, we aimed to evaluate indoor air quality (IAQ) versus the use of K and LPG heaters inside a test room reflecting the typical conditions of Jordanian dwellings during the winter season. The IAQ was evaluated with portable aerosol monitors to measure the particle number concentrations and size distribution within a wide particle diameter range of 0.01–25 μm. We utilized a simple sectional indoor aerosol model (SIAM) to estimate the emission rate and lifetime of the combustion products in the test room.

2. Materials and Methods

2.1. Measurement Setup

2.1.1. Instrumentation

The measurement setup consisted of two condensation particle counters (CPC, 3007-2 and P-Trak 8525, Shoreview, TSI, MI, USA) and a handheld optical particle counter (AeroTrak 9306-V2, Shoreview, TSI, MI, USA). The use of portable aerosol instruments has been growing. Their performance was evaluated in the laboratory, in the field, or by side-by-side comparison with more reliable instruments [50–56].

The CPC measured the total submicron particle number concentration, and it had a cut-off size of 10 nm; the sampling flow rate was 0.1 lpm (inlet flow rate 0.7 lpm); maximum detectable concentration was ~10⁵ cm⁻³ with 20% accuracy. The P-Trak is a similar particle counter; its cut-off size was 25 nm; and its maximum concentration was 5 × 10⁵ cm⁻³. The CPC and the P-Trak were operated with a 1 s time resolution. The AeroTrak measured size-specific particle number concentrations (optical diameter range was 0.3–25 μm; 6-channels user-defined). The channels were set at 0.3, 0.5, 1, 2.5, 10, and 25 μm. The sampling time resolution was 30 s at a flow rate of 2.83 lpm.

The measurement was performed inside an office ($5 \times 3 \times 3 \text{ m}^3$) on the second floor of the Department of Physics (University of Jordan, Amman, Jordan). The room was naturally ventilated, and included full furniture (desk, tables, chairs, window curtains, etc.). The office was kept closed during the sampling, i.e., the window and door were closed during the measurement session. The door was opened briefly (less than a couple of seconds), to access the instruments for routine checkup. The instruments were set up on a table about 75 cm height from the floor, in the middle of the office.

2.1.2. Data Handling

The aerosol database was harmonized, and concentrations were averaged with 1 min time resolution. The particle number size distribution was generated by merging the data obtained from the above-mentioned three portable instruments. It was possible to have eight channels:

- 10–25 nm (the difference between the CPC and the P-Trak)
- 25–300 nm (the difference between the P-Trak and the Aerotrak)
- Six channels taken directly from the AeroTrak (0.3–0.5 μm , 0.5–1 μm , 1–2.5 μm , 2.5–5 μm , 5–10 μm , and 10–25 μm)

The size-fractionated number concentrations were calculated by integrating (practical summation) the lognormal particle number size distribution over the specified particle diameter range:

$$PN_{D_{p1}-D_{p2}} = \int_{D_{p1}}^{D_{p2}} n_N^0 \cdot d\log_{10}(D_p) \quad (1)$$

where $n_N^0 = dN/d\log_{10}(D_p)$ was the lognormal particle number size distribution. Similarly, the size-fractionated mass concentrations were calculated by integrating the lognormal particle mass size distribution:

$$PM_{D_{p1}-D_{p2}} = \int_{D_{p1}}^{D_{p2}} n_M^0 \cdot d\log_{10}(D_p) \quad (2)$$

where $n_M^0 = dM/d\log_{10}(D_p)$ was the lognormal particle mass size distribution. The particles were assumed to be spherical, with unit density of ($\rho_p = 1000 \text{ kg/m}^3$). In other words, the lognormal particle mass size distribution was calculated as follows:

$$n_M^0 = \frac{dM}{d\log_{10}(D_p)} = \frac{dN}{d\log(D_p)} \frac{\pi}{6} D_p^3 \rho_p = n_N^0 \frac{\pi}{6} D_p^3 \rho_p \quad (3)$$

2.2. Heating Combustion Scenarios

The heating combustion scenarios consisted of the operation of the most commonly used natural gas and kerosene heaters in Jordan. Many different types of kerosene and natural gas heaters are used in Jordan. They vary in shape, size, and combustion rate. The heaters in this study were carefully selected to ensure the most commonly used type. The model and image of the selected heaters were omitted from this study, to safeguard the manufacturers' privacy.

2.2.1. Natural Gas Heater

The natural gas heater (about $42 \times 36 \times 72 \text{ cm}^3$) was a "3-burner portable cabinet LPG indoor natural gas room heater". It was made of a metal frame with a compartment for a 15-kg gas bottle, which was installed from the rear. The front side consisted of the burner panels, which provided three heat settings—minimum, medium, and maximum—providing heat output of 1.5, 2.9, and 4.2 kW, respectively. The corresponding heat consumption was, respectively, 110, 210, and 305 g/h.

We conducted three test Scenarios, one for each heat setting (minimum, medium, and maximum). The first Scenario started with one panel (minimum setting) turned

on for about an hour, then turned off. The air inside the room was then allowed to return to its background concentration level as it had been measured before starting the heater. The second and third Scenarios were done in a similar way, but with the heat set at medium (two panels) and maximum (three panels), respectively. These alternating Scenarios allowed us to obtain an estimated value for the total particle loss, which was used to correct for the emission rates during the two alternating Scenarios.

2.2.2. Kerosene Heater

There are many kerosene heater designs. They can be categorized into two main types, based on how the fuel is burned: (1) wick heaters, that rely on the capillary transfer of fuel (2) vapor-jet nozzle burners, that aerosolize the fuel using manual pumping or heat. The vapor-jet nozzle burner is more efficient and hotter, but the nozzle can get clogged by soot, whereas wick stoves are more commonly used because they are cheaper.

The selected kerosene heater was a middle-size type (about $33 \times 33 \times 48 \text{ cm}^3$), that had a circular shape. The tank (capacity $\sim 5.5 \text{ L}$) was in the bottom, and the combustion part was sheltered with a round mesh. A cover cap was installed on top of the round mesh. The combustion part consisted of a wick with an adjustable setting to provide variable heat output. The fuel consumption was about 0.25 L/h , providing a heat output of about 8000 BTU/h .

We conducted two test scenarios:

- Scenario 1: the heater was ignited inside the room, and allowed to reach its maximum heat. It operated at its maximum heat for about one hour, and then it was taken out of the room until the indoor aerosols concentrations returned to their pre-Scenario 1 level (this took 1.5 h).
- Scenario 2: the heater was ignited outdoors until it reached its maximum heat, and was then taken inside the room to operate for about one hour. Then, it was taken back outside, and the indoor aerosols concentrations were left to reach their pre-Scenario 2 background level.

As with the natural gas heater alternating scenarios, these alternating scenarios for the kerosene heater enabled an estimated value to be obtained for the total particle loss, which was used to correct for the emission rates during the two alternating scenarios.

2.3. Simple Indoor Aerosol Model

Indoor aerosols can be of an indoor or outdoor origin. However, in our combustion scenarios of natural gas and kerosene heaters, the indoor aerosol sources were the primary concern, being predominant. Eventually, the emitted aerosols were either deposited onto surfaces or removed from the indoor air via air exchange with the outdoor air. Aerosol particles also undergo complex processes through aerosol dynamics and chemical reactions that change their state, concentration, and physical–chemical properties; however, we ignored this, because the resolution of the measured particle number size distribution was too coarse to observe the effects of coagulation, condensation, and chemical reactions.

The dynamic behavior of indoor aerosols can be described by the mass balance equation [57,58]. A simple indoor aerosol model (IAM) describes the dynamic behavior of a single component (e.g., total aerosol particle number concentration) inside a single compartment (i.e., a single zone). A sectional indoor aerosol model (SIAM) describes the dynamic behavior of the aerosol population by handling each particle size bin separately or interactively with other size bins (i.e., in case of the evolution of aerosols via coagulation, condensation, etc.).

Here, we applied a simplified form of the SIAM mass balance equation:

$$\frac{dI_i}{dt} = P_i \lambda O_i - (\lambda + \lambda_{d,i}) I_i + S_{in,i} \quad (4)$$

where t is the time; I and O are the indoor and outdoor concentrations, respectively, of the aerosol particles; P is the penetration factor of the aerosol particles while being transported

from the outdoor air into the indoor air; λ is the ventilation rate; λ_d is the deposition rate of the aerosol particles onto the available indoor surfaces and S_{in} represents the emission rates from an indoor source. The subscript i indicates that the mass balance equation is valid for a certain particle size range (i.e., particle size channel).

Well-mixed indoor air is the assumption, for the mass balance equation to be valid [57]. Otherwise, spatial variation of indoor aerosol particle concentrations must be taken into account by, for example, utilizing computational fluid dynamic (CFD) models. The assumption was valid in our room, because its size was small enough for the heat convection from the convection source to mix the indoor air efficiently. Therefore, the sampled aerosols were assumed to be convected from the source to the instruments in less than one minute.

With further assumptions as outlined in the following two sections, we utilized the simplified form of the SIAM to estimate the total particle loss inside the test room, and the emission rates of the aerosols originated from the combustion process during the operation of the heaters.

2.3.1. Particle Losses

The second term on the right-hand side of Equation (4) represents the total particle loss via dry deposition and removal by ventilation. Immediately after an indoor source is stopped, Equation (4) can be rewritten as:

$$\frac{dI_i}{dt} = -(\lambda + \lambda_{d,i})I_i \quad (5)$$

Here, it is assumed that the indoor aerosols from indoor origin are dominant (i.e., $P\lambda O \ll (\lambda + \lambda_d)I$). As such, the decaying concentration can be fitted to Equation (5) to obtain an estimate for the total particle losses: $-(\lambda + \lambda_{d,i})$.

2.3.2. Emission Rates

The third term on the right-hand side of Equation (4) represents the emission rate from an indoor source. If this term is the dominant parameter (i.e., $S_{in} \ll P\lambda O - (\lambda + \lambda_d)I$), then we can rewrite Equation (4) as:

$$\frac{dI_i}{dt} = S_{in,i} \quad (6)$$

However, Equation (6) might underestimate the emission rate if the particle loss term $(\lambda + \lambda_d)$ is comparable to the source term (S_{in}). Therefore, a more accurate approach is to correct for the particle loss, which are estimated according to the previous section. As such, Equation (6) becomes:

$$S_{in,i} = \frac{dI_i}{dt} + \{(\lambda + \lambda_{d,i})I_i\}_{empirical} \quad (7)$$

3. Results and Discussion

3.1. Total Particle Concentrations and Particle Size Distributions

The total particle number concentration during the natural gas operation clearly reflected the burner settings at minimum, medium, and maximum (i.e., 1, 2, and 3 panels). As an example, the total particle number concentrations are illustrated in Figure 1a for one of the measurement sessions. During Scenario I (i.e., 1-panel operation), the concentrations varied within the range 6×10^4 – 2.4×10^5 cm^{-3} . It was expected that the concentration level would double or triple during Scenario II (i.e., 2-panel operation) or Scenario III (i.e., 3-panel operation), but their levels were within the ranges 1.6×10^5 – 3.5×10^5 cm^{-3} and 2.8×10^5 – 5.9×10^5 cm^{-3} , respectively.

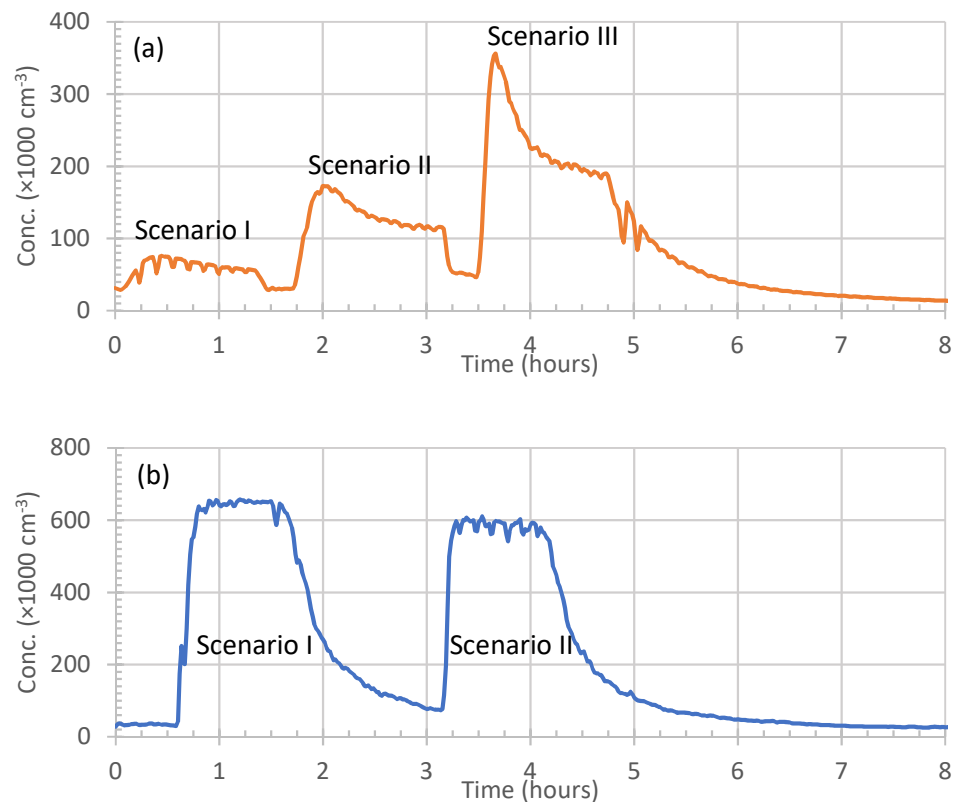


Figure 1. Measurement session examples reflecting the particle number concentrations observed during the operation of (a) natural gas heater scenarios and (b) kerosene heater scenarios. The scenarios are explained in Section 2.2 above.

The two kerosene heater operation scenarios had concentrations higher (Figure 1b) than those observed during the natural gas heater scenarios (Figure 1a). They ranged between $4 \times 10^5 \text{ cm}^{-3}$ and $8 \times 10^5 \text{ cm}^{-3}$, with relatively higher concentrations during Scenario I (i.e., igniting the heater inside the room) than during Scenario II (i.e., igniting the heater outside the room).

The observed particle number size distribution during the natural gas heater operation was characterized by high concentrations in the first two particle size channels, i.e., particles with diameter ranges 10–25 nm and 25–300 nm (Figure 2). Interestingly, the increase in concentrations was more pronounced in the first particle size channel, reflecting the significant amount of secondary particle formation during the combustion of natural gas. The more heat output (number of burner panels in operation), the more concentrations measured in those two channels.

The observed particle number size distributions during the kerosene heater operation were also characterized by high concentrations in the first two particle size channels (Figure 3). When compared to the natural gas size distributions, kerosene heating was accompanied with significantly high concentrations in the second particle size channel; this indicated soot aerosols formation due to incomplete combustion of kerosene.

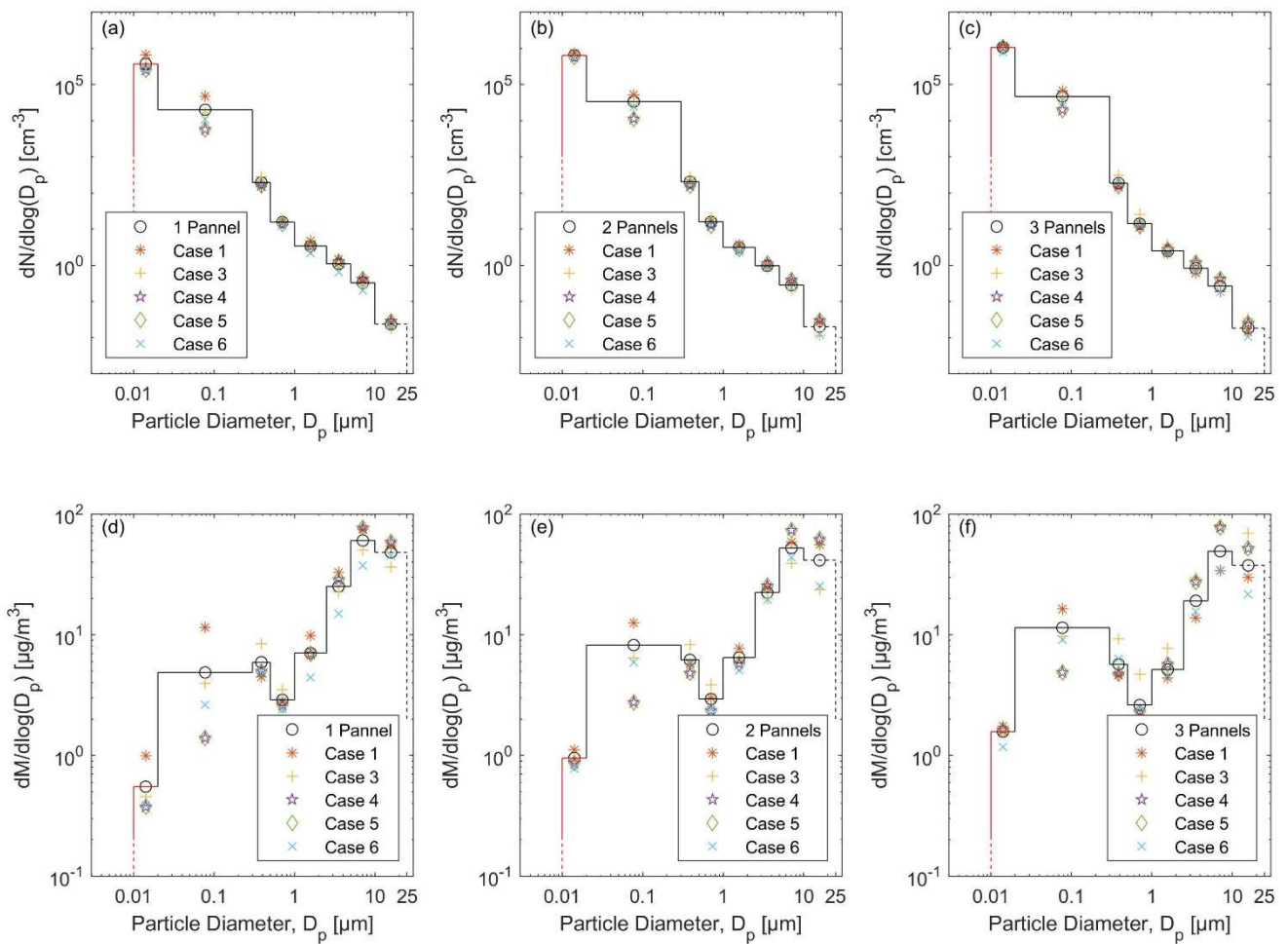


Figure 2. Particle number size distributions observed during the natural gas heater operation with (a) one panel, (b) two panels, and (c) three panels, and the corresponding particle mass size distribution (d–f).

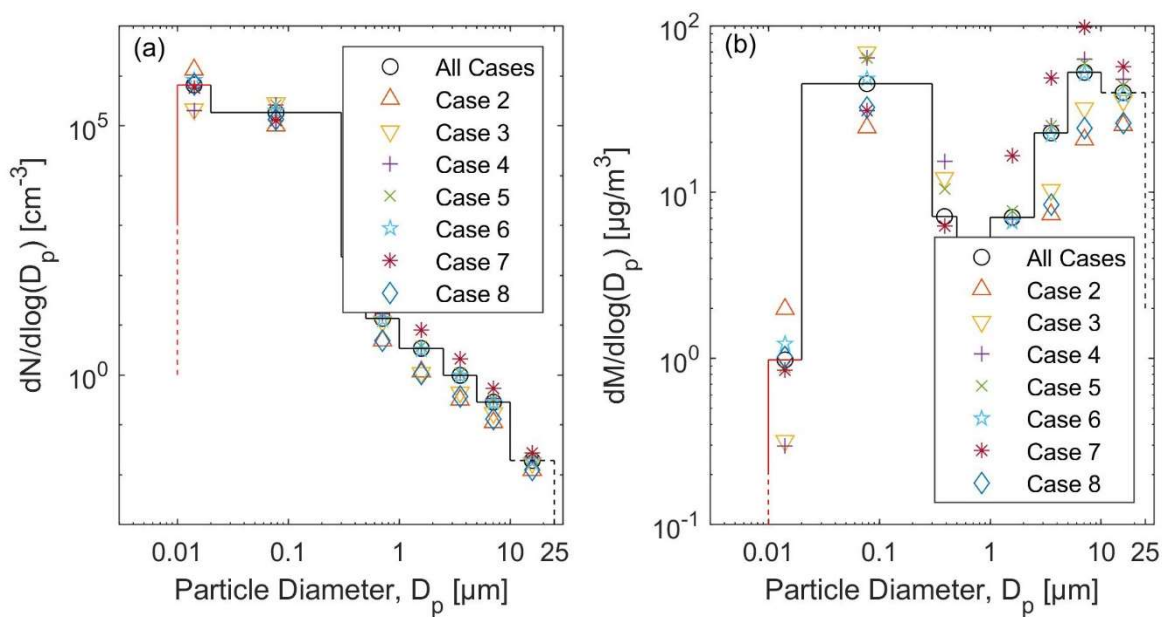


Figure 3. (a) Particle number size distributions observed during the kerosene heater operation and (b) corresponding particle mass size distributions.

The ratio between the particle number size distributions during the operation of the heaters, and that of the background conditions, was about 2–3 orders of magnitude (Figure 4).

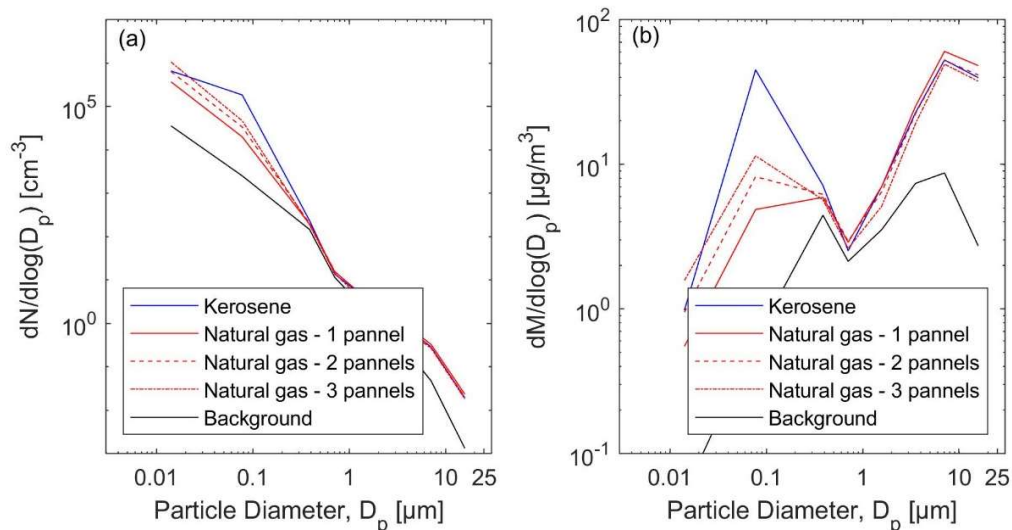


Figure 4. (a) Overall mean particle number size distributions observed during the operation of the heaters, compared with the background size distributions, and (b) corresponding particle mass size distributions.

3.2. Particle Losses

The total loss of the aerosol particles was calculated for each particle size channel (Figure 5). On average, it was 0.7–1.6 h⁻¹ for micron particles (1–10 μm) and 0.8–0.9 h⁻¹ for ultrafine particles (<0.1 μm). For particles within the diameter range 0.3–1 μm, the total particle loss was 0.5–0.6 h⁻¹, which is an upper estimate for the average ventilation rate of the test room, because dry deposition was least in that particle size range. The U-shape of the total particle losses agrees well with the theory of the three-layer deposition model [59].

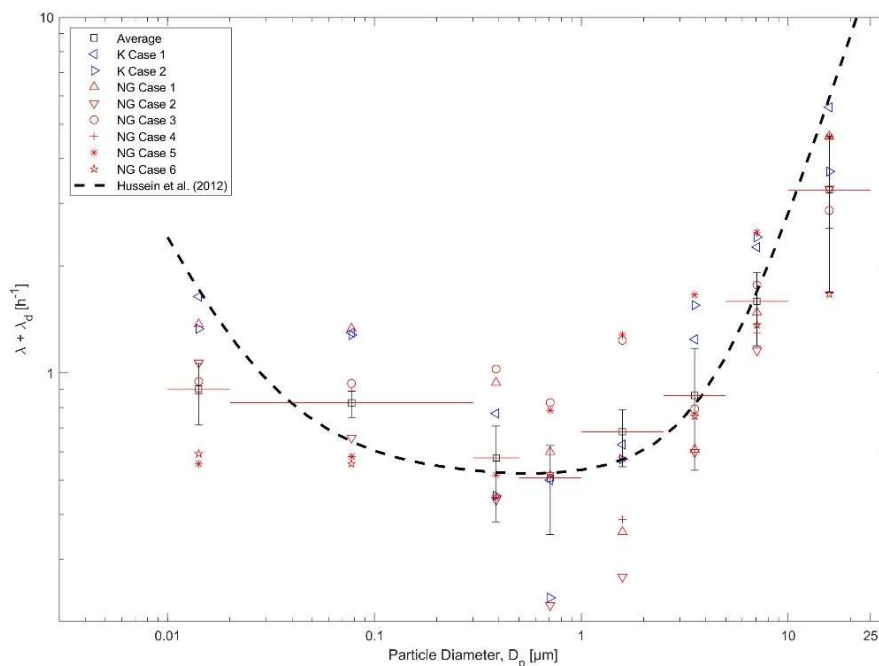


Figure 5. An average estimation for the total particle loss inside the test room compared with the three-layer model calculation (Hussein, et al. [59]).

3.3. Emission Rates

3.3.1. The Natural Gas Heater Scenarios

Recalling the example illustrated in Figure 1a for the three scenarios of the natural gas heater operation, we can postulate that the source term $S_{in,i}$ was overriding the mass balance equation during the initial stage, leading to the sudden increase in the indoor particle concentrations. The indoor particle concentrations reached steady-state a short time after the start of the scenario. During the increasing stage of the indoor concentrations, the emission rate was estimated according to Equation (6).

Applying Equation (6) revealed that the emission rate during the first stage of the scenarios emitted ultrafine particles with an average emission rate as high as 1.2×10^{10} , 1.9×10^{10} , and 2.8×10^{10} particles/s, respectively, during the first stage of each scenario. The corresponding particle number and mass size distributions of the emission rates are presented in Figure 6.

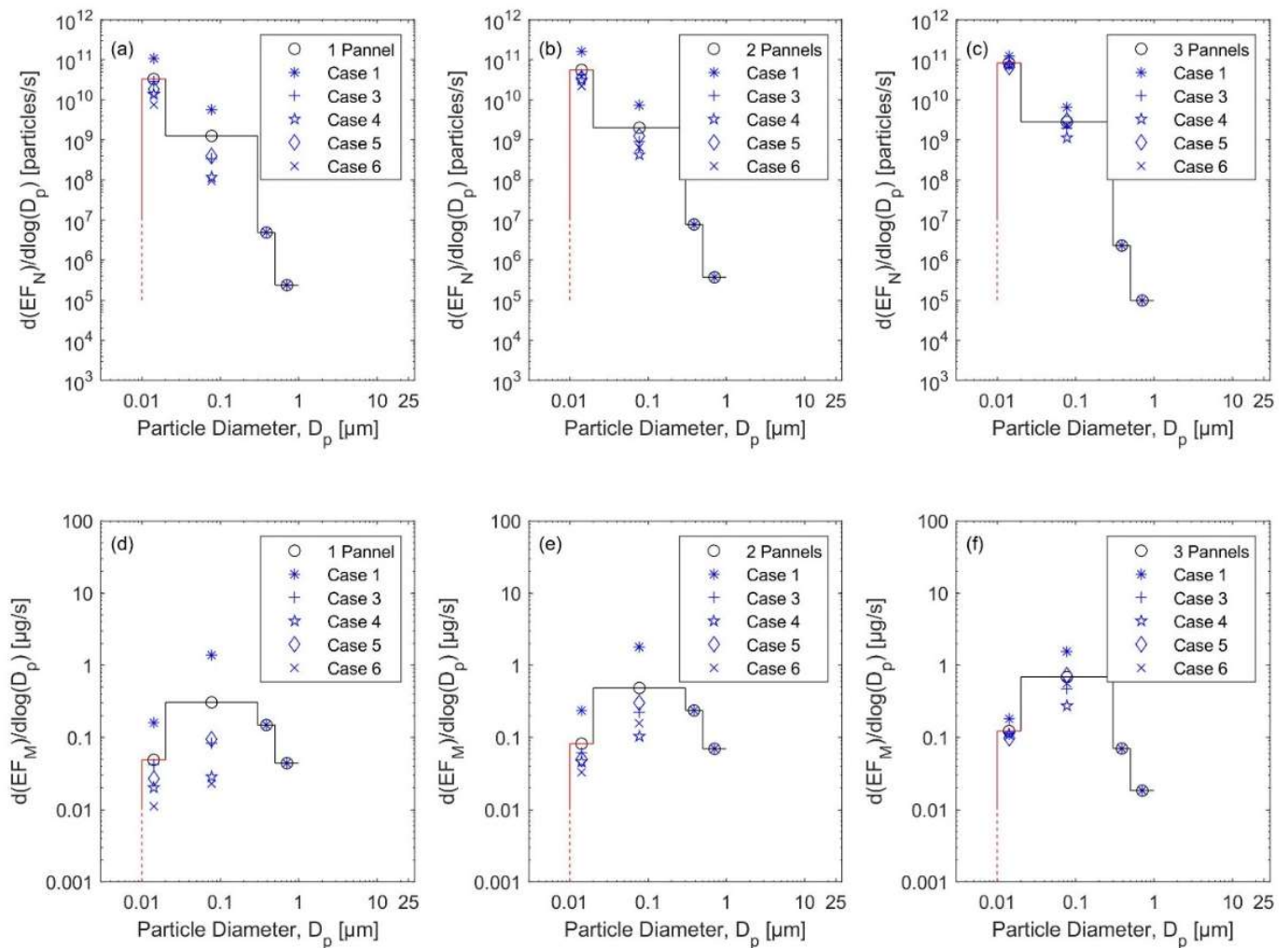


Figure 6. The emission rates during the three scenarios of the natural gas heater operation, presented in the form of (a–c) particle number size distributions and (d–f) particle mass size distributions.

During the steady-state condition, the sources were balanced by the sinks. Assuming $(\lambda + \lambda_d)I \gg P\lambda O$, then Equation (4) reads:

$$[S_{in,i} \approx (\lambda + \lambda_{d,i})I_i]_{steady-state} \tag{8}$$

and gives an average steady-state emission rate of 3.6×10^9 , 6.1×10^9 , and 10.1×10^9 particles/s, respectively, for each scenario. These were apparently about one order of magnitude lower than those observed during the initial stage of each scenario.

According to the manufacturer specifications for the natural gas heater, the heat output was 1.5, 2.9, or 4.2 kW, and the heat consumption was 110, 210, and 305 g/h, respectively, for the operation settings at one, two, or three panels during steady-state conditions. This led to the conclusion that the average amount of particles emitted was 2.1×10^6 – 2.4×10^6 particles/J or 1.1×10^{11} – 1.2×10^{11} particles/g during steady-state conditions. During heating-up (i.e., the first stage of each scenario) this was 6.6×10^6 – 8.0×10^6 particles/J or 3.3×10^{11} – 3.9×10^{11} particles/g.

3.3.2. The Kerosene Heater Scenarios

As illustrated for the kerosene heater scenarios in Figure 1b, the source term $S_{in,i}$ was overriding the mass balance equation during the initial stage, leading to a sudden increase in the indoor particle concentrations. The indoor particle concentrations reached steady-state a very short time after the start of the scenario. During the increasing stage of the indoor concentrations, the average emission rates were about 4.4×10^{10} particles/s for both scenarios; the corresponding particle number and mass size distributions of the emission rates are presented in Figure 7. During the steady-state stage, the average emission rates were about 6.2×10^9 particles/s and 5.0×10^9 particles/s, respectively, for each scenario. As a comparison with the emission rates obtained during the natural gas heater operation, the emission rates observed during the kerosene heater operation were higher (Figure 8).

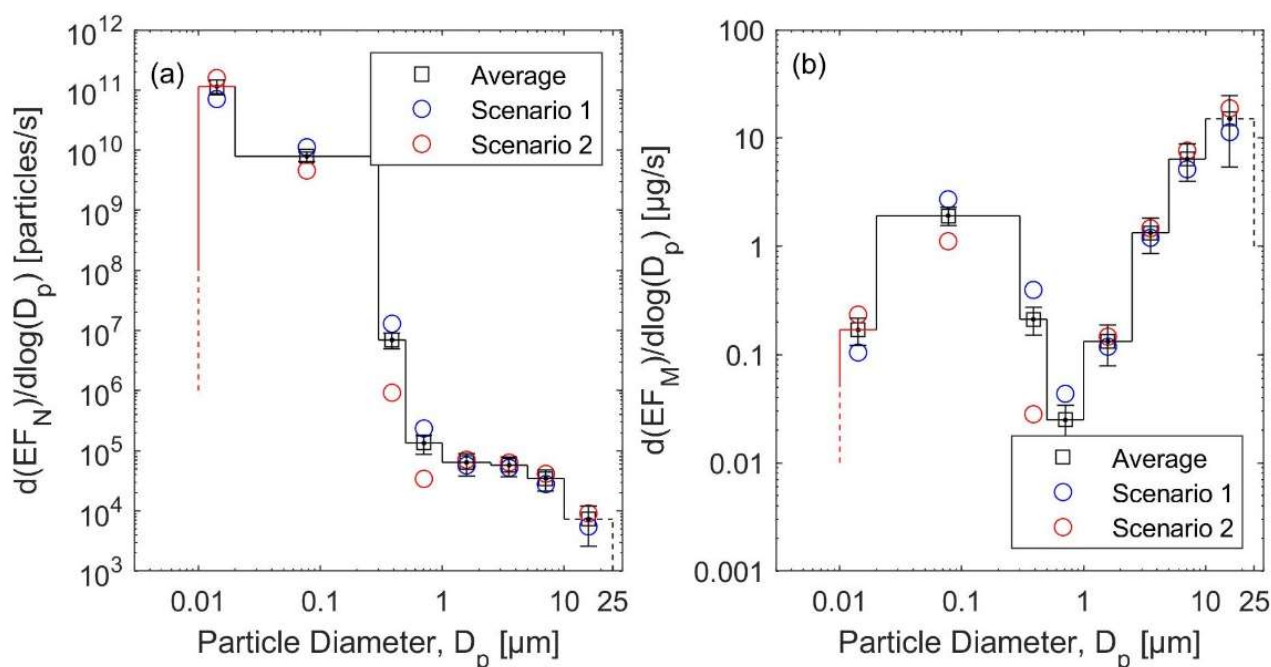


Figure 7. The emission rates during the two scenarios of the kerosene heater operation presented in the form of (a) particle number size distributions and (b) particle mass size distributions.

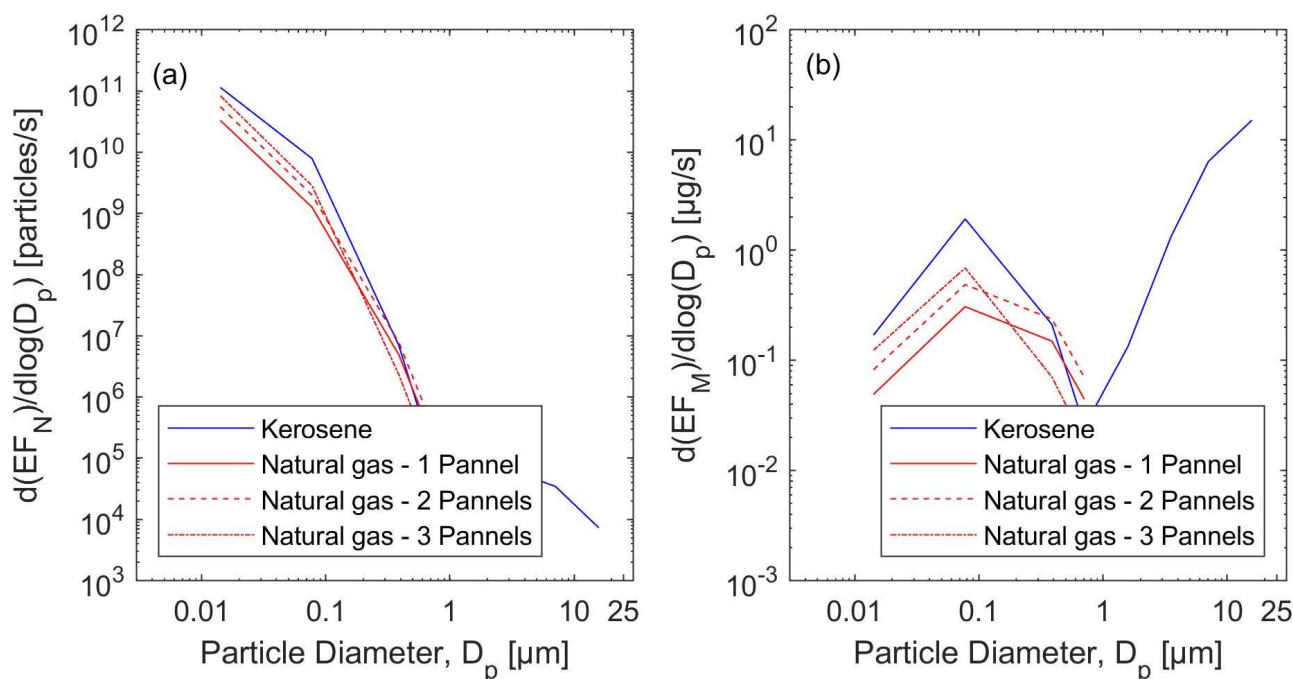


Figure 8. The overall emission rates during all scenarios of the heaters' operation, presented in the form of (a) particle number size distributions and (b) particle mass size distributions.

According to the manufacturer specifications for the kerosene heater, the heat output was 8000 BTU/h (≈ 2.35 kW) and the heat consumption was 0.25 L/h during steady-state conditions. This led to the conclusion that the average amount of particles emitted was 2.1×10^6 – 2.6×10^6 particles/J or 0.9×10^{11} – 1.1×10^{11} particles/g (assuming density of kerosene 0.8 g/cm^3) during the steady-state conditions. During the heating-up stage, this was about 1.9×10^7 particles/J or about 7.9×10^{11} particles/g.

Collectively, the results suggest that Jordanian indoor environments can be heavily polluted during the winter when compared to the surrounding outdoor atmosphere, primarily due to the ubiquity of indoor combustion associated with heating. Although K and LPG heaters are widely used in the Eastern Mediterranean region, there have been very few studies of their impact on the indoor air quality [48,60,61]. Jodeh, et al. [61] performed a measurement campaign in Nablus City, which is an important urban and industrial center in Palestine, to evaluate the IAQ at four roadsides versus four urban homes in Nablus. Alsbou and Omari [60] focused on evaluating BTEX (benzene, toluene, ethylbenzene, and xylene isomers) in indoor air environments during the winter, generated by commonly used heaters in Jordan (diesel pot-bellied heater with chimney; electric heater; unfluted gas heater; K heater; and wood pot-bellied heater with chimney) showing that K heaters were the most polluting heater based on BTEX measurement. All these studies concluded that the use of heating combustion significantly influences the IAQ, especially in the winter season.

Hussein, et al., [48] evaluated the IAQ in Jordanian urban dwellings (eight dwellings in Amman) during the winter versus the summer season, and reported that the use of K and LPG heaters had a significant negative impact on the IAQ. The particle number (PN) and particle mass (PM) size distributions varied with the different indoor emission sources, and among the eight dwellings tested by Hussein, et al. [48] in Amman, Jordan. Natural gas cooking and natural gas or kerosene heaters were associated with PN concentrations in the order of 100,000 to 400,000 cm^{-3} , and $\text{PM}_{2.5}$ concentrations often in the range of 10–150 $\mu\text{g/m}^3$. Indoor cooking (using LPG cookers) and combustion processes were also found to increase concentrations of carbon monoxide, nitrogen dioxide, and volatile organic compounds. In general, concentrations of indoor particles were lower during the summer compared to the winter as a result of the use of combustion processes indoors during the

winter and, at the same time, tightly closed indoor environments to store heat. Following a quick check for the influence of indoor activities (e.g., combustion processes indoors) on the IAQ indoors, Hussein, et al., [48] reported that the PN concentrations were generally below 10^4 cm^{-3} .

This study is important, because in Jordan about 61% of the total residential energy consumption is consumed for heating spaces using portable unflued K and LPG stoves [25]. According to their representative survey of 106 low–middle income households in urban Amman, Younis, et al., [25] showed that unflued K and LPG heaters were used for heating spaces by around 39% and 89%, respectively. Almost 65% of them used more than one device for heating their dwelling. Around 50% of those households reported different health problems related to asthma. Almost 75% of households lived in apartments constructed with external envelopes of hollow cement blocks, leading to poor fabric performance. The use of K and LPG as a heating source is not limited to households in Jordan; it is also widely used in commercial and public service buildings such as unclassified hotels, some clinics and health centers, and retail shops [62]. Recently, Ahmed, et al. [24] recommended a set of interventions to improve the IAQ based on enhanced performance of the energy consumption of residential buildings in Jordan: (1) orientation of the buildings for enhanced thermal benefit; (2) window-size-to-wall-area ratios for optimized ventilation, and (3) insulation, for enhanced heat saving. If these factors were to be taken into account, the need for combustion sources as a heat source could be reduced significantly.

4. Conclusions

About 61% of the total residential energy consumption in Jordan is consumed for heating spaces using portable kerosene (K) and liquified petroleum gas (LPG) heaters. Therefore, the indoor air quality (IAQ) is significantly affected by combustion processes used for household heating during the winter.

In this study, we evaluated the IAQ versus the use of K and LPG heaters inside a test room reflecting the typical conditions of Jordanian dwellings during the winter season. The experimental set-up included measurement of the particle size distribution (diameter 0.01–25 μm) using portable monitors: two condensation particle counters (CPC, 3007-2 and P-Trak 8525) and a handheld optical particle counter (AeroTrak 9306-V2). We utilized a simple sectional indoor aerosol model (SIAM) to estimate the emission rate and lifetime of the combustion products in the test room.

On average, the particle loss was $0.7\text{--}1.6 \text{ h}^{-1}$ for micron particles (1–10 μm) and $0.8\text{--}0.9 \text{ h}^{-1}$ for ultrafine particles (<0.1 μm). An upper estimate for the ventilation rate was taken from the loss rate of particles 0.3–1 μm in diameter, showing a value around $0.5\text{--}0.6 \text{ h}^{-1}$, which is typical for a closed room with natural ventilation.

The LPG heater operated with three different settings: minimum (one panel), medium (two panels), and maximum (three panels). The particle number (PN) concentration during the LPG operation was within the range $6 \times 10^4\text{--}5.9 \times 10^5 \text{ cm}^{-3}$, depending on the setting (minimum, medium, or maximum). The emission rate from the LPG heater was $1.2 \times 10^{10}\text{--}2.8 \times 10^{10}$ particles/s ($6.6 \times 10^6\text{--}8.0 \times 10^6$ particles/J) during the heating-up stage, and $3.6 \times 10^9\text{--}10.1 \times 10^9$ particles/s ($2.1 \times 10^6\text{--}2.4 \times 10^6$) during the steady-state stage.

During the K heater operation, the PN concentrations were within the range $4 \times 10^5\text{--}8 \times 10^5 \text{ cm}^{-3}$. The corresponding emission rate was about 4.4×10^{10} particles/s (1.9×10^7 particles/J) during the heating-up stage. During the steady-state operation, the average emission rate was $5.0 \times 10^9\text{--}6.2 \times 10^9$ particles/s ($6.6 \times 10^6\text{--}8.0 \times 10^6$ particles/J).

The results call for an immediate need to apply interventions to improve the IAQ by turning to cleaner heating processes in Jordanian households.

Author Contributions: Conceptualization, T.H.; methodology, T.H., O.A.-J., N.B. and B.Z.; software, T.H.; validation, T.H., O.A.-J., N.B., B.Z. and B.L.; formal analysis, T.H., O.A.-J., N.B. and B.Z.; investigation, T.H., O.A.-J., N.B., B.Z. and B.L.; resources, T.H.; data curation, T.H., O.A.-J., N.B. and B.Z.; writing—original draft preparation, T.H.; writing—review and editing, T.H., O.A.-J., N.B., B.Z. and B.L.; visualization, T.H., O.A.-J., N.B. and B.Z.; supervision, T.H., O.A.-J. and B.L.; project administration, T.H.; funding acquisition, T.H. All authors have read and agreed to the published version of the manuscript.

Funding: This research was financially supported by generous funding from the Deanship of Scientific Research at the University of Jordan (grant #2379) and the Scientific Research Support Fund at the Jordanian Ministry of Higher Education (project #WE-2-2-2017).

Institutional Review Board Statement: Not applicable.

Informed Consent Statement: Not applicable.

Data Availability Statement: Data is available upon request.

Acknowledgments: The authors acknowledge the support of the Deanship of Scientific Research (DSR) at the University of Jordan. T.H. acknowledges the support of the Scientific Research Support Fund at the Jordanian Ministry of Higher Education; the Atmosphere and Climate Competence Center (ACCC) Flagship funded by the Academy of Finland (grant #337549); and the Eastern Mediterranean and Middle East Climate and Atmosphere Research (EMME-CARE) project, which received funding from the European Union's Horizon 2020 Research and Innovation Programme (Grant Agreement Number 856612) and the Government of Cyprus. The sole responsibility of this publication lies with the authors. Open access funding was provided by the University of Helsinki.

Conflicts of Interest: The authors declare no conflict of interest.

References

- Schilmann, A.; Ruiz-García, V.; Serrano-Medrano, M.; de la Sierra de la Vega, L.A.; Olaya-García, B.; Estevez-García, J.A.; Berrueta, V.; Horacio Riojas-Rodríguez, H.; Masera, O. Just and fair household energy transition in rural Latin American households: Are we moving forward? *Environ. Res. Lett.* **2021**, *16*, 105012. [[CrossRef](#)]
- Vardoulakis, S.; Giagloglou, E.; Steinle, S.; Davis, A.; Sleenwenhoek, A.; Galea, K.S.; Dixon, K.; Crawford, J.O. Indoor Exposure to Selected Air Pollutants in the Home Environment: A Systematic Review. *Int. J. Environ. Res. Public Health* **2020**, *17*, 8972. [[CrossRef](#)]
- Lam, N.L.; Smith, K.R.; Gauthier, A.; Bates, M.N. Kerosene: A review of household uses and their hazards in low- and middle-income countries. *J. Toxicol. Environ. Health Part B* **2012**, *15*, 396–432. [[CrossRef](#)]
- Leaderer, B.P.; Naeher, L.; Jankun, T.; Balenger, K.; Holford, T.R.; Toth, C.; Sullivan, J.; Wolfson, J.M.; Koutrakis, P. Indoor, outdoor, and regional summer and winter concentrations of PM₁₀, PM_{2.5}, SO₄²⁻, H⁺, NH₄⁺, NO₃⁻, NH₃, and nitrous acid in homes with and without kerosene space heaters. *Environ. Health Perspect.* **1999**, *107*, 223–231. [[CrossRef](#)]
- Leaderer, B.P. Air pollutant emissions from kerosene space heaters. *Science* **1982**, *218*, 1113–1115. [[CrossRef](#)]
- Leaderer, B.P.; Zgraniski, R.T.; Berwick, M.; Stolwijk, J.A. Assessment of exposure to indoor air contaminants from combustion sources: Methodology and application. *Am. J. Epidemiol.* **1986**, *124*, 275–289. [[CrossRef](#)]
- Ruiz, P.A.; Toro, C.; Caceres, J.; Lopez, G.; Oyola, P.; Koutrakis, P. Effect of gas and kerosene space heaters on indoor air quality: A study in homes of Santiago, Chile. *J. Air Waste Manag. Assoc.* **2010**, *60*, 98–108. [[CrossRef](#)]
- Kliucininkas, L.; Martuzevicius, D.; Krugly, E.; Prasauskas, T.; Kauneliene, V.; Molnar, P.; Strandberg, B. Indoor and outdoor concentrations of fine particles, particle-bound PAHs and volatile organic compounds in Kaunas, Lithuania. *J. Environ. Monit.* **2011**, *13*, 182–191. [[CrossRef](#)]
- Villanueva, F.; Tapia, A.; Amo-Salas, M.; Notario, A.; Cabañas, B.; Martínez, E. Levels and sources of volatile organic compounds including carbonyls in indoor air of homes of Puertollano, the most industrialized city in central Iberian Peninsula. Estimation of health risk. *Int. J. Hyg. Environ. Health* **2015**, *218*, 522–534. [[CrossRef](#)]
- Alexopoulos, E.C.; Chatzis, C.; Linos, A. An analysis of factors that influence personal exposure to toluene and xylene in residents of Athens, Greece. *BMC Public Health* **2006**, *6*, 50. [[CrossRef](#)]
- Lee, J.H.; Lee, H.S.; Park, M.R.; Lee, S.W.; Kim, E.H.; Cho, J.B.; Kim, J.; Han, Y.; Jung, K.; Cheong, H.K.; et al. Relationship between indoor air pollutant levels and residential environment in children with atopic dermatitis. *Allergy Asthma Immunol. Res.* **2014**, *6*, 517–524. [[CrossRef](#)]
- Ferrero, A.; Esplugues, A.; Estarlich, M.; Llop, S.; Cases, A.; Mantilla, E.; Ballester, F.; Iñiguez, C. Infants' indoor and outdoor residential exposure to benzene and respiratory health in a Spanish cohort. *Environ. Pollut.* **2017**, *222*, 486–494. [[CrossRef](#)]
- Adgate, J.L.; Church, T.R.; Ryan, A.D.; Ramachandran, G.; Fredrickson, A.L.; Stock, T.H.; Morandi, M.T.; Sexton, K. Outdoor, indoor, and personal exposure to VOCs in children. *Environ. Health Perspect.* **2004**, *112*, 1386–1392. [[CrossRef](#)]

14. Phillips, M.L.; Esmen, N.A.; Hall, T.A.; Lynch, R. Determinants of exposure to volatile organic compounds in four Oklahoma cities. *J. Expo. Anal. Environ. Epidemiol.* **2005**, *15*, 35–46. [[CrossRef](#)]
15. Gillespie-Bennett, J.; Pierse, N.; Wickens, K.; Crane, J.; Nicholls, S.; Shields, D.; Boulic, M.; Viggers, H.; Baker, M.; Woodward, A.; et al. Sources of nitrogen dioxide (NO₂) in New Zealand homes: Findings from a community randomized controlled trial of heater substitutions. *Indoor Air* **2008**, *18*, 521–528. [[CrossRef](#)]
16. Lim, Y.-H.; Hersoug, L.-G.; Lund, R.; Bruunsgaard, H.; Ketznel, M.; Brandt, J.; Jeanette Jørgensen, T.; Westendorp, R.; Andersen, Z.J.; Loft, S. Inflammatory markers and lung function in relation to indoor and ambient air pollution. *Int. J. Hyg. Environ. Health* **2022**, *241*, 113944. [[CrossRef](#)]
17. Belanger, K.; Triche, E.W. Indoor Combustion and Asthma. *Immunol. Allergy Clin. N. Am.* **2008**, *28*, 507–519. [[CrossRef](#)]
18. Triche, E.W.; Belanger, K.; Bracken, M.B.; Beckett, W.S.; Holford, T.R.; Gent, J.F.; McSharry, J.-E.; Leaderer, B.P. Indoor Heating Sources and Respiratory Symptoms in Nonsmoking Women. *Epidemiology* **2005**, *16*, 377–384. [[CrossRef](#)]
19. Chen, L.C.; Qu, Q.; Gordon, T. Respiratory Effects of Kerosene Space Heater Emissions. *Inhal. Toxicol.* **1996**, *8*, 49–64. [[CrossRef](#)]
20. Fullerton, D.G.; Bruce, N.; Gordon, S.B. Indoor air pollution from biomass fuel smoke is a major health concern in the developing world. *Trans. R. Soc. Trop. Med. Hyg.* **2008**, *102*, 843–851. [[CrossRef](#)]
21. Fullerton, D.G.; Jere, K.; Jambo, K.; Kulkarni, N.S.; Zijlstra, E.E.; Grigg, J.; French, N.; Molyneux, M.E.; Gordon, S.B. Domestic smoke exposure is associated with alveolar macrophage particulate load. *Trop. Med. Int. Health* **2009**, *14*, 349–354. [[CrossRef](#)]
22. Apple, J.; Vicente, R.; Yarberr, A.; Lohse, N.; Mills, E.; Jacobson, A.; Poppendieck, D. Characterization of particulate matter size distributions and indoor concentrations from kerosene and diesel lamps. *Indoor Air* **2010**, *20*, 399–411. [[CrossRef](#)]
23. Sahu, M.; Peipert, J.; Singhal, V.; Yadama, G.N.; Biswas, P. Evaluation of mass and surface area concentration of particle emissions and development of emissions indices for cookstoves in rural India. *Environ. Sci. Technol.* **2011**, *45*, 2428–2434. [[CrossRef](#)]
24. Ahmed, M.; Al-Khashman, O.A.; Al-Shrideh, A.Z. The Optimal Use of Renewable Energy in Residential Buildings Under Jordanian Building Regulation: A Case Study. *Int. J. Energy Convers.* **2021**, *9*. [[CrossRef](#)]
25. Younis, A.; Taki, A.; Bhattacharyya, S. Sustainability issues in low-middle income apartments in urban Amman, Jordan: Heating devices and health concerns. *WIT Trans. Built Environ.* **2020**, *193*, 27.
26. Ruiz-Mercado, I.; Maser, O.; Zamora, H.; Smith, K.R. Adoption and sustained use of improved cookstoves. *Energy Policy* **2011**, *39*, 7557–7566. [[CrossRef](#)]
27. Kawamoto, T.; Matsuno, K.; Arashidani, K.; Yoshikawa, M.; Kayama, F.; Kodama, Y. Personal Exposure to Nitrogen Dioxide from Indoor Heaters and Cooking Stoves. *Arch. Environ. Contam. Toxicol.* **1993**, *25*, 534–538.
28. Changa, W.R.; Chenga, C.L. Carbon monoxide transport in an enclosed room with sources from a water heater in the adjacent balcony. *Built. Environ.* **2008**, *43*, 861–870. [[CrossRef](#)]
29. Carteret, M.; Pauwels, J.-F.; Hanoune, B. Emission factors of gaseous pollutants from recent kerosene space heaters and fuels available in France in 2010. *Indoor Air* **2012**, *22*, 299–308. [[CrossRef](#)]
30. Arashidani, K.; Yoshikawa, M.; Kawamoto, T.; Matsuno, K.; Kayama, F.; Kodama, Y. Indoor Pollution from Heating. *Ind. Health* **1996**, *34*, 205–215.
31. Bozzelli, J.W.; Kebbekus, B.; Bobenhausen, C. Analysis of selected volatile organic compounds associated with residential kerosene heater use. *Int. J. Environ. Stud.* **1995**, *49*, 125–131. [[CrossRef](#)]
32. Chambon, C.; Schadkowski, C. Impact of Kerosene Portable Heaters on Indoor Carbon Monoxide Concentrations. *Pollut. Atmos.* **2005**, *1*, 103–106.
33. Ristovski, Z.D.; Tas, I.; Morawska, L.; Saxby, W. Investigation into the emission of fine particles, formaldehyde, oxides of nitrogen and carbon monoxide from natural gas heaters. *J. Aerosol Sci.* **2000**, *31* (Suppl. S1), S490–S491. [[CrossRef](#)]
34. Uchiyama, S.; Tomizawa, T.; Tokoro, A.; Aoki, M.; Hishiki, M.; Yamada, T.; Tanaka, R.; Sakamoto, H.; Yoshida, T.; Bekki, K.; et al. Gaseous chemical compounds in indoor and outdoor air of 602 houses throughout Japan in winter and summer. *Environ. Res.* **2015**, *137*, 364–372. [[CrossRef](#)]
35. Hansel, N.; McCormack, M.; Belli, A.; Matsui, E.; Peng, R.; Aloe, C.; Paulin, L.; Williams, D.A.; Diette, G.; Breyse, P. In-home air pollution is linked to respiratory morbidity in former smokers with COPD. *Am. J. Respir. Crit. Care Med.* **2013**, *187*, 1085–1090. [[CrossRef](#)]
36. Dong, J.I.; Banerjee, K.; Bozzelli, J.W. Total hydrocarbon pollutants from a non-vented radiant kerosene heater. *Int. J. Environ. Stud.* **1988**, *32*, 75–83. [[CrossRef](#)]
37. Apte, M.G.; Traynor, G.W.; Froehlich, D.A.; Sokol, H.A.; Porter, W.K. The impact of add-on catalytic devices on pollutant emissions from unvented kerosene heaters. *J. Air Pollut. Control Assoc.* **1989**, *39*, 1228–1230. [[CrossRef](#)]
38. Cheng, Y.-S.; Zhou, Y.; Chow, J.; Watson, J.; Frazier, C. Chemical composition of aerosols from kerosene heaters burning jet fuels. *Aerosol Sci. Technol.* **2001**, *35*, 949–957. [[CrossRef](#)]
39. Lionel, T.; Martin, R.J.; Brown, N.J. A comparative study of combustion in kerosene heaters. *Environ. Sci. Technol.* **1986**, *20*, 78–85. [[CrossRef](#)]
40. Traynor, G.W.; Allen, J.R.; Apte, M.G.; Girman, J.R.; Hollowell, C.D. Pollutant emissions from portable kerosene fired space heaters. *Environ. Sci. Technol.* **1983**, *17*, 369–371. [[CrossRef](#)]
41. Traynor, G.W.; Apte, M.G.; Carruthers, A.R.; Dillworth, J.F.; Grimsrud, D.T.; Thompson, W.T. Indoor air pollution and inter-room pollutant transport due to unvented kerosene-fired space heaters. *Environ. Int.* **1987**, *13*, 159–166. [[CrossRef](#)]

42. Traynor, G.W.; Apte, M.G.; Sokol, H.A.; Chuang, J.C.; Tucker, W.G.; Mumford, J.L. Selected organic pollutant emissions from unvented kerosene space heaters. *Environ. Sci. Technol.* **1990**, *24*, 1265–1270. [[CrossRef](#)]
43. Yamanaka, S.; Hirose, H.; Takada, S. Nitrogen oxide emissions from domestic kerosene-fired and gas-fired appliances. *Atmos. Environ.* **1979**, *13*, 407–412. [[CrossRef](#)]
44. Yamanaka, S. Decay rates of nitrogen oxides in a typical Japanese living room. *Environ. Sci. Technol.* **1984**, *18*, 566–570. [[CrossRef](#)]
45. Zhou, Y.; Cheng, Y. Characterization of emissions from kerosene heaters in an unvented tent. *Aerosol Sci. Technol.* **2000**, *33*, 510–524. [[CrossRef](#)]
46. Adgate, J.; Reid, H.F.; Helms, R.W.; Berg, R.A. Nitrogen dioxide and urinary excretion of hydroxyproline and desmosine. *Arch. Environ. Health* **1992**, *47*, 376–384. [[CrossRef](#)]
47. Mumford, J.L.; Williams, R.W.; Walsh, D.B.; Burton, R.M.; Svendsgaard, D.J.; Chuang, J.C.; Houk, V.S.; Lewtas, J. Indoor air pollutants from unvented kerosene heater emissions in mobile homes: Studies on particles, semivolatile organics, carbon monoxide, and mutagenicity. *Environ. Sci. Technol.* **1991**, *25*, 1732–1738. [[CrossRef](#)]
48. Hussein, T.; Alameer, A.; Jaghbeir, O.; Albeitshaweesh, K.; Malkawi, M.; Boor, B.E.; Koivisto, A.J.; Löndahl, J.; Alrifai, O.; Al-Hunaiti, A. Indoor Particle Concentrations, Size Distributions, and Exposures in Middle Eastern Microenvironments. *Atmosphere* **2020**, *11*, 41. [[CrossRef](#)]
49. Khumsaeng, T.; Kanabkaew, T. Measurement of Indoor Air Pollution in Bhutanese Households during Winter: An Implication of Different Fuel Uses. *Sustainability* **2021**, *13*, 9601. [[CrossRef](#)]
50. Wang, X.; Chancellor, G.; Evenstad, J.; Farnsworth, J.; Hase, A.; Olson, G.; Sreenath, A.; Agarwal, J. A novel optical instrument for estimating size segregated aerosol mass concentration in real time. *Aerosol Sci. Technol.* **2009**, *43*, 939–950. [[CrossRef](#)]
51. Maricq, M.M. Monitoring Motor Vehicle PM Emissions: An Evaluation of Three Portable Low-Cost Aerosol Instruments. *Aerosol Sci. Technol.* **2013**, *47*, 564–573. [[CrossRef](#)]
52. Chung, A.; Chang, D.P.Y.; Kleeman, M.J.; Perry, K.; Cahill, T.A.; Dutcher, D.; McDougal, E.M.; Stroud, K. Comparison of real-time instruments used to monitor airborne particulate matter. *J. Air Waste Manag. Assoc.* **2001**, *51*, 109–120. [[CrossRef](#)] [[PubMed](#)]
53. Nyarku, M.; Mazaheri, M.; Jayaratne, R.; Dunbabin, M.; Rahman, M.M.; Uhde, E.; Morawska, L. Mobile phones as monitors of personal exposure to air pollution: Is this the future? *PLoS ONE* **2018**, *13*, e0193150. [[CrossRef](#)] [[PubMed](#)]
54. Cheng, Y.H.; Lin, M.H. Real-time performance of the micro-aeth AE51 and the effects of aerosol loading on its measurement results at a traffic site. *Aerosol Air Qual. Res.* **2013**, *13*, 1853–1863. [[CrossRef](#)]
55. Cai, J.; Yan, B.; Ross, J.; Zhang, D.; Kinney, P.L.; Perzanowski, M.S.; Jung, K.; Miller, R. and Chillrud, S.N. Validation of MicroAeth® as a black carbon monitor for fixed-site measurement and optimization for personal exposure characterization. *Aerosol Air Qual. Res.* **2014**, *14*, 1–9. [[CrossRef](#)]
56. Hämeri, K.; Koponen, I.K.; Aalto, P.P.; Kulmala, M. The particle detection efficiency of the TSI3007 condensation particle counter. *Aerosol Sci.* **2002**, *33*, 1463–1469. [[CrossRef](#)]
57. Hussein, T.; Kulmala, M. Indoor aerosol modeling: Basic principles and practical applications. *Water Air Soil Pollut. Focus* **2007**, *8*, 23–34. [[CrossRef](#)]
58. Nazaroff, W.W. Indoor Particle Dynamics. *Indoor Air* **2004**, *14*, 175–183. [[CrossRef](#)]
59. Hussein, T.; Smolik, J.; Kerminen, V.-M.; Kulmala, M. Modeling dry deposition of aerosol particles onto rough surfaces. *Aerosol Sci. Technol.* **2012**, *46*, 44–59. [[CrossRef](#)]
60. Alsbou, E.M.; Omari, K.W. BTEX indoor air characteristic values in rural areas of Jordan: Heaters and health risk assessment consequences in winter season. *Environ. Pollut.* **2020**, *267*, 115464. [[CrossRef](#)]
61. Jodeh, S.; Hasan, A.R.; Amarah, J.; Judeh, F.; Salghi, R.; Lgaz, H.; Jodeh, W. Indoor and outdoor air quality analysis for the city of Nablus in Palestine: Seasonal trends of PM₁₀, PM_{5.0}, PM_{2.5}, and PM_{1.0} of residential homes. *Air Qual. Atmos. Health* **2018**, *11*, 229–237. [[CrossRef](#)]
62. Jaber, J.O.; Mohsen, M.S.; Al-Sarkhi, A.; Akash, B. Energy analysis of Jordan's commercial sector. *Energy Policy* **2003**, *31*, 887–894. [[CrossRef](#)]